JACS
JOURNAL OF THE AMERICAN CHEMICAL SOCIETY
pubs.acs.org/JACS
Communication

Structural Characterization of the $[CuOR]^{2+}$ Core

V. Mahesh Krishnan,[§] Dimitar Y. Shopov,[§] Caitlin J. Bouchey, Wilson D. Bailey, Riffat Parveen, Bess Vlaisavljevich,* and William B. Tolman*

Cite This: *J. Am. Chem. Soc.* 2021, 143, 3295−3299
Read Online
ACCESS | Metrics & More | Article Recommendations | Supporting Information

ABSTRACT: Formal Cu(III) complexes bearing an oxygen-based auxiliary ligand ($[CuOR]^{2+}$, R = H or CH_2CF_3) were stabilized by modulating the donor character of supporting ligand L^Y (L^Y = 4-Y, *N*,*N*′-bis(2,6-diisopropylphenyl)-2,6-pyridinedicarboxamide, Y = H or OMe) and/or the basicity of the auxiliary ligand, enabling the first characterization of these typically highly reactive cores by NMR spectroscopy and X-ray crystallography. Enhanced lifetimes in solution and slowed rates of PCET with a phenol substrate were observed. NMR spectra corroborate the *S* = 0 ground states of the complexes, and X-ray structures reveal shortened Cu−ligand bond distances that match well with theory.

Understanding the molecular structures, spectroscopic properties, and reactivity of copper−oxygen complexes[1−5] is important for gaining insight into the mechanisms by which copper enzymes and other catalysts function.[6,7] Among the various complexes studied, those comprising the $[CuOH]^{2+}$ core supported by dicarboxamide ligands (Figure 1)[8−14] are notably reactive, attacking C−H and O−H bonds

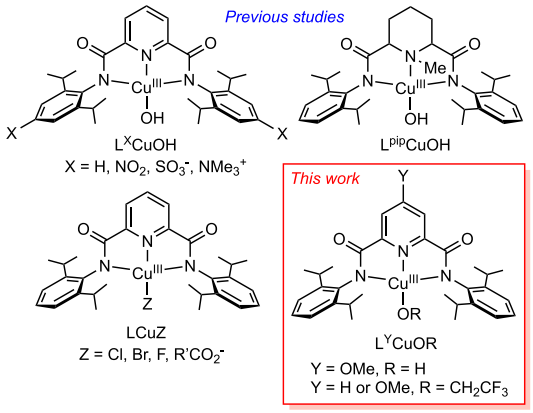

Figure 1. Complexes studied previously and the compounds that comprise the focus of this work. R′ = Me or aryl groups.

via proton-coupled electron transfer (PCET) processes and undergoing electron transfer at high rates (cf. the rate constant for the reaction of L^HCuOH with 1,2-dihydroanthracene 50 M^{-1} s^{-1} at −25 °C;[9] electron-transfer self-exchange rate constant ~10^4 M^{-1} s^{-1} at −88 °C[13]). The formulations of the complexes are supported by UV−vis spectroscopy (diagnostic absorptions with ligand-to-metal charge-transfer (LMCT) character), EPR silence, resonance Raman spectroscopy (ν_{Cu-O} ≈ 630 cm^{-1}),[13] EXAFS (avg Cu−N,O ≈ 0.1 Å shorter than for the $[Cu^{II}OH]^+$ precursor),[8] and theory.[8,15]

Perturbations of the $[CuOH]^{2+}$ core have been effected by the installation of remote substituents on the flanking aryl rings (L^XCuOH, Figure 1).[11,12] These perturbations are reflected by shifts in the LMCT energies (lower), redox potentials (higher), basicities (lower), and PCET reaction rates (faster) that may be rationalized by electron withdrawal by the X groups. Changing the pyridyl group to a piperidine ($L^{pip}CuOH$) has the opposite effects, attributed to greater electron donation by the amine donor. In no case has a complex with the $[CuOH]^{2+}$ core been structurally defined by X-ray crystallography, in large part due to its high reactivity and poor thermal stability ($t_{1/2}$ ≈ minutes at −80 °C in THF). These characteristics and the fact that decomposition yields paramagnetic Cu(II) species have also inhibited efforts to obtain NMR spectra that would be useful in confirming the proposed *S* = 0 ground state. Significantly slower reactions and greater stability were observed for the LCuZ derivatives (Z = halide[8,16] or carboxylate[17]) featuring a less-basic X-type reactive moiety, of which the halide complexes were characterized recently by X-ray diffraction and NMR spectroscopy.[16] Inspired by that success, we hypothesized that more complete characterization of the $[CuOH]^{2+}$ core might be attained if its stability could be enhanced. Toward this end, we targeted two modifications: the placement of an electron-donating *para*-methoxy pyridyl group (Y = OMe; L^{OMe}) and the use of a less-basic alkoxide moiety ($CF_3CH_2O^-$). On the basis of previous work,[9,11,12] we hypothesized that these changes would enhance the solution stability, thereby facilitating handling and characterization. We now report the confirmation of these hypotheses through the synthesis of the targeted derivatives and their characterization by X-ray crystallography and NMR spectroscopy, which with comparison to results from theory provides new insights into the

Received: January 2, 2021
Published: February 23, 2021

https://dx.doi.org/10.1021/jacs.0c13470
J. Am. Chem. Soc. 2021, 143, 3295−3299

molecular and electronic structures of complexes with $[CuOH]^{2+}$ and $[CuOCH_2CF_3]^{2+}$ cores.

The reaction of proligand H_2L^{OMe} with $Cu(OTf)_2$ in the presence of NaOMe and CH_3CN led to the isolation of key precursor $L^{OMe}Cu(CH_3CN)$ (77%), which upon treatment with NBu_4OH led to $[NBu_4][L^{OMe}CuOH]$ (76%). $[NBu_4][L^{Y}CuOCH_2CF_3]$ (Y = H or OMe) complexes were obtained from the respective hydroxide precursors via protonolysis with $HOCH_2CF_3$. The complexes $L^{OMe}Cu(CH_3CN)$, $[NBu_4][L^{OMe}CuOH]$, and $[NBu_4][L^{Y}CuOCH_2CF_3]$ (Y = H or OMe) were characterized by UV−vis and X-band EPR spectroscopy, CHN analysis, and X-ray crystallography (SI). The complexes feature a slightly distorted square-planar geometry (τ_4 = 0.15−0.22)[18] with Cu−N,O bond distances typical for such Cu(II) species (Figures S43−S45; Table 1) and characteristic S = 1/2 rhombic signals with Cu and N hyperfine patterns in EPR spectra (Figures S7−S9).

Table 1. Bond Distances (Å) Obtained by X-ray Crystallography for $[CuOR]^{2+}$ (Cu^{III}) and $[CuOR]^{+}$ (Cu^{II}) Species and by DFT Geometry Optimization for $[CuOR]^{2+}$ (Theory)[a]

bond	species	L^{OMe}, OH	L^{H}, OCH_2CF_3	L^{OMe}, OCH_2CF_3
Cu−N_2	Cu^{III}	1.841(3)	1.864(13)	1.856(3)
	theory	*1.845*	*1.875*	*1.866*
	Cu^{II}	1.927(2)	1.925(4)	1.927(1)
	Cu^{III}−Cu^{II}	−0.086	−0.061	−0.071
Cu−$N_{1,3}$	Cu^{III}	1.900(3)	1.950(12)	1.948(3)
	theory	*1.916*	*1.960*	*1.960*
	Cu^{II}	2.027(2)	2.058(4)	2.020(1)
	Cu^{III}−Cu^{II}	−0.127	−0.108	−0.072
Cu−O_1	Cu^{III}	1.799(3)	1.812(12)	1.849(5)
	theory	*1.783*	*1.818*	*1.817*
	Cu^{II}	1.867(2)	1.857(4)	1.838(2)
	Cu^{III}−Cu^{II}	−0.068	−0.045	0.011
mean	Cu^{III}−Cu^{II}	−0.102	−0.081	−0.051

[a]Averaged values are presented for carboxamide Cu−N_1 and Cu−N_3 bonds. N_2 is pyridyl donor. Estimated standard deviations are in parentheses.

The expected electronic perturbations of the L^{OMe} and $-OCH_2CF_3$ moieties are reflected in cyclic voltammograms (THF, 0.2 M Bu_4NPF_6), which contain quasi-reversible waves associated with $[CuOR]^{2+}/[CuOR]^{+}$ couples (Table 2). Good reversibility of the waves for the $-OCH_2CF_3$ complexes is apparent at scan rates as slow as 10 mV/s (Figure S20), consistent with low reactivity for the oxidized species (*vide infra*). A more modest enhancement of reversibility is seen for $[NBu_4][L^{OMe}CuOH]$ relative to the analog supported by L^{H} (Figure S18).[5] The replacement of −OH with $-OCH_2CF_3$ shifts the $E_{1/2}$ by +0.191 V on average, whereas the alteration of L^{Y} had a lesser effect, with an average difference of only −0.049 V induced by the introduction of the *p*-OMe substituent.

Table 2. Reduction Potentials for the $[CuOR]^{2+/+}$ Couple and Rate Constants for Reactions with ^{ttb}PhOH

compound	$E_{1/2}$ (mV)[a]	k_2 (M^{-1} s^{-1})[b]
$L^{H}CuOH$	−167[c]	15 900
$L^{OMe}CuOH$	−202	11 800
$LCuOCH_2CF_3$	+37	3.0
$L^{OMe}CuOCH_2CF_3$	−25	1.5

[a]Conditions: THF, 0.2 M Bu_4NPF_6, values vs $Fc^{+/0}$. [b]Conditions: −25 °C in DFB using either 1 equiv ($L^{Y}CuOH$) or 50 equiv ($L^{Y}CuOCH_2CF_3$). [c]This value is ∼100 mV lower than reported previously under the same conditions,[11] which we ascribe to the previous use of external Fc referencing rather than the internal referencing used herein. (See SI IV for details.)

The chemical oxidation of $[NBu_4][L^{OMe}CuOH]$ or $[NBu_4][L^{Y}CuOCH_2CF_3]$ (Y = H or OMe) was performed by adding 1 equiv of $FcBAr^{F}_4$ or $AcFcBArF_4$, respectively, in THF (−80 °C) or in 1,2-difluorobenzene (DFB, −25 °C). Immediate color changes (deep violet or blue) and intense electronic absorption features (Figure 2) diagnostic of the formation of

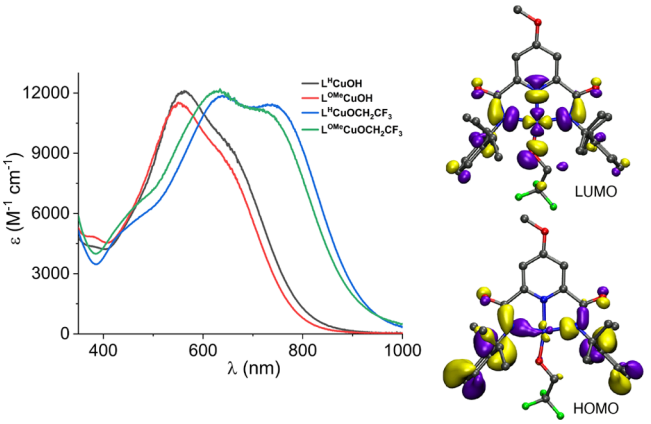

Figure 2. (Left) UV−visible absorption spectra of the indicated compounds in DFB at −25 °C. (Right) Orbitals for $L^{OMe}CuOCH_2CF_3$ plotted with an isovalue of 0.04 au from the B98 functional.

$[CuOH]^{2+}$ and $[CuOCH_2CF_3]^{2+}$ cores were observed, and reversible one-electron processes were confirmed through titrations and the sequential cyclic additions of oxidant and decamethylferrocene (Figures S22−S27).[13] TDDFT UV−vis transitions exhibit λ_{max} values in agreement with experiment that are predominantly HOMO to LUMO (Figure 2) and shift from 546.1 and 537.1 nm in $L^{H}CuOH$ and $L^{OMe}CuOH$ to 578.7 and 573.6 nm in $L^{H}CuOCH_2CF_3$ and $L^{OMe}CuOCH_2CF_3$, respectively, as a result of the stabilization of the LUMO (Table S4, Figures S50−S58). Also in agreement with experiment (and precedent[17a]), additional transitions with partial HOMO-to-LUMO character contribute at longer wavelengths to the spectra for the $-OCH_2CF_3$ complexes. Resonance Raman spectra of frozen solutions (λ_{ex} = 561 nm) of all $L^{Y}CuOR$ complexes contain a signal at ∼635 cm^{-1} that we assign as $\nu_{Cu\text{-}OR}$ by analogy to data acquired for $L^{H}CuOH$ and theory (Figures S45−S49 and S59, Table S15).[13]

To evaluate how ligand variation influences stability and reactivity, we compared the reactions of $L^{Y}CuOH$ and $L^{Y}CuOCH_2CF_3$ (Y = H or OMe) with 2,4,6-tri-*tert*-butylphenol (^{ttb}PhOH) to yield the stable phenoxyl radical.[11,19,20] Second-order rate constants were measured using either 1 equiv ($L^{Y}CuOH$) or 50 equiv ($L^{Y}CuOCH_2CF_3$) of ^{ttb}PhOH at −25 °C in DFB (Table 2). The data show significantly higher reactivity for the hydroxide complexes (≳5000-fold), a difference that may be attributed to the higher basicity of the −OH vs $-OCH_2CF_3$ moieties and/or steric inhibition for the latter. Modest decreases in the rate constants

https://dx.doi.org/10.1021/jacs.0c13470
J. Am. Chem. Soc. 2021, 143, 3295−3299

for the cases where Y = OMe at parity for −OR may be rationalized by stabilization of the $[CuOR]^{2+}$ core by the electron-donating methoxide substituent. Monitoring the room-temperature decays of the four $[CuOR]^{2+}$ species in the absence of substrate in THF and DFB revealed complicated kinetic traces, but trends in the overall lifetimes paralleled the ^{ttb}PhOH reactivity trends (SI; cf. $t_{1/2} \approx 4$ h vs <1 h for $L^{OMe}CuOCH_2CF_3$ vs LCuOH in DFB).

The enhanced stability of the new complexes led us to attempt characterization by X-ray crystallography. We discovered that the complex prepared by the treatment of $[NBu_4][L^{OMe}CuOH]$ with $FcBAr^F{}_4$ in DFB could be isolated as suitable deep-purple crystals via the layered diffusion of pentane at −30 °C. Similar attempts with $[NBu_4][L^YCuOCH_2CF_3]$ (Y = H or OMe) failed to give suitable crystals, likely in part due to the formation of highly intractable viscous residues containing $[NBu_4][BAr^F{}_4]$. To circumvent this issue, we employed reactants that would yield insoluble inorganic salts as byproducts. Thus, we reacted $LCu(CH_3CN)$[4] and $L^{OMe}Cu(CH_3CN)$ with $NaOCH_2CF_3$ and then oxidized the resulting crude materials with $AcFcSbF_6$ in CH_2Cl_2 or DFB. After the removal of a light-colored precipitate (presumably $NaSbF_6$), suitable crystals of the oxidized products were obtained at −30 °C.

Representations of the X-ray structures of $L^{OMe}CuOH$ and $L^{OMe}CuOCH_2CF_3$ (Figure 3) as well as $L^HCuOCH_2CF_3$

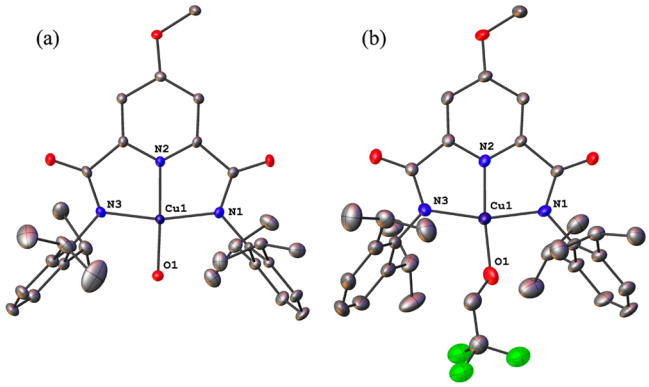

Figure 3. Representations of the X-ray structures of (a) $L^{OMe}CuOH$ and (b) $L^{OMe}CuOCH_2CF_3$, showing all nonhydrogen atoms as 50% thermal ellipsoids.

(Figure S42) show similar square-planar geometries compared to their $[CuOR]^+$ progenitors (τ_4 = 0.11−0.15), but they are neutral species as expected for one-electron oxidation products. Comparison of metal−ligand bond distances between the oxidized and reduced forms (Table 1) indicates in all but one case shortening upon oxidation, by as much as 0.127 Å. The average Cu−N/O bond contraction in $L^{OMe}CuOH$, 0.102 Å, is in excellent agreement with previously reported EXAFS analyses of L^HCuOH (0.1 Å).[8] The trifluoroethoxides show somewhat less contraction and in $L^{OMe}CuOCH_2CF_3$ the Cu−O bond even lengthens slightly, by 0.011 Å, but disorder in the trifluoroethoxide ligand imparts an inherent inaccuracy to the O atom's position. Gas-phase geometry optimizations (SI) for the S = 0 ground states of the oxidized species are in excellent agreement with the experimentally determined values (*theory* in Table 1). Overall, the bond length differences between the precursor and oxidation products are consistent with the loss of an electron from orbitals spanning the Cu center and/or its immediate environment, as reported for less-reactive complexes LCuZ (Z = F, Cl, Br).[16] Furthermore, the lack of significant structural changes associated with this redox event agrees with the low reorganization energy of 0.95 eV previously measured for the $[L^HCuOH]^-/L^HCuOH$ couple.[14]

While theoretical calculations support a closed-shell S = 0 ground state for the $[CuOH]^{2+}$ core (Table S5),[8] the only experimental corroboration has come from a dearth of signal in the X-band EPR spectrum, an observation consistent with either the S = 0 or S = 1 ground state. Acquiring NMR spectra, which would distinguish the two spin states, presents challenges due to the formation of paramagnetic Cu(II) decay species. We were nonetheless able to observe sharp peaks in the diamagnetic region of ^{1}H NMR spectra for both L^YCuOH species in 1,2-dichlorobenzene-d_4 at −15 °C (Figure S28−S29), although broadening due to decomposition was evident for Y = H. The ^{1}H NMR spectrum of the more robust complex $L^HCuOCH_2CF_3$ in THF-d_8 at −80 °C (Figure S30) displayed negligible broadening, but some resonances were obscured by solvent/byproduct signals. Since $L^{OMe}CuOCH_2CF_3$ could be isolated in neat form as a crystalline solid, NMR spectra of isolated material were collected (CD_2Cl_2, −15 °C), and all expected ^{1}H NMR resonances and J couplings (Figure 4) as well as $^{13}C\{^1H\}$

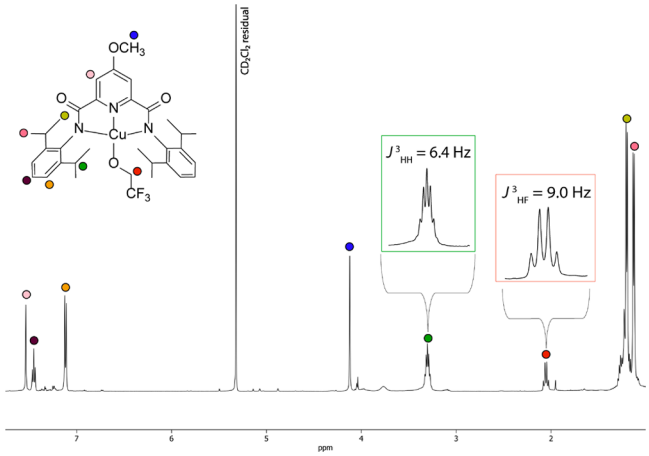

Figure 4. ^{1}H NMR spectrum of $L^{OMe}CuOCH_2CF_3$ (CD_2Cl_2, −15 °C).

NMR peaks (Figure S32) were observed. The sharpness of the observed ^{1}H and $^{13}C\{^1H\}$ NMR features in the diamagnetic chemical shift region confirms an S = 0 ground state, in agreement with predictions.[8]

In conclusion, we prepared and characterized a new set of complexes with $[CuOR]^{+/2+}$ cores using a modified supporting ligand and/or core (R = CH_2CF_3). Both changes attenuate the PCET reactivity of the oxidized state, the former by lowering its oxidizing potential and the latter by lowering the basicity of the proton-accepting site. While each modification has the opposite effect on the opposite property (e.g., the less-basic proton acceptor also leads to a more oxidizing species), the dominant impact is on electronics for the supporting ligand and basicity for the core, in line with previously observed reactivity trends and demonstrating how PCET reactivity can be tuned. These stabilization effects were sufficient to permit, for the first time, the successful characterization of complexes with $[CuOR]^{2+}$ cores by X-ray crystallography and NMR

https://dx.doi.org/10.1021/jacs.0c13470
J. Am. Chem. Soc. 2021, 143, 3295−3299

spectroscopy. These data are consistent with several predictions made about $L^{H}CuOH$, in particular, the conservation of geometry with minimal reorganization upon oxidation,[14] the EXAFS-derived contraction of Cu−L bonds by ∼0.1 Å on oxidation,[8] the calculated geometries, and the diamagnetic $S = 0$ ground state.[8] To the best of our knowledge, the complexes with R = CH_2CF_3 are the first alkoxo analogs bearing the formal Cu(III) oxidation state, and with the discovery that they share many similarities with their hydroxide counterparts, including PCET reactivity with phenols, the potential for steric and electronic tuning that is unavailable with hydroxide makes this class of compounds promising for further research into the bond-activation properties of high-valent copper species.

■ ASSOCIATED CONTENT

Supporting Information

The Supporting Information is available free of charge at https://pubs.acs.org/doi/10.1021/jacs.0c13470.

DFT structural coordinate file (XYZ)
Experimental details and figures (PDF)

Accession Codes

CCDC 2053118−2053123 contain the supplementary crystallographic data for this paper. These data can be obtained free of charge via www.ccdc.cam.ac.uk/data_request/cif, or by emailing data_request@ccdc.cam.ac.uk, or by contacting The Cambridge Crystallographic Data Centre, 12 Union Road, Cambridge CB2 1EZ, UK; fax: +44 1223 336033.

■ AUTHOR INFORMATION

Corresponding Authors

Bess Vlaisavljevich − *University of South Dakota, Vermillion, South Dakota 57069, United States;* orcid.org/0000-0001-6065-0732; Email: bess.vlaisavljevich@usd.edu

William B. Tolman − *Department of Chemistry, Washington University in St. Louis, St. Louis, Missouri 63130-4899, United States;* orcid.org/0000-0002-2243-6409; Email: wbtolman@wustl.edu

Authors

V. Mahesh Krishnan − *Department of Chemistry, Washington University in St. Louis, St. Louis, Missouri 63130-4899, United States;* orcid.org/0000-0001-9642-5908

Dimitar Y. Shopov − *Department of Chemistry, Washington University in St. Louis, St. Louis, Missouri 63130-4899, United States;* orcid.org/0000-0002-4689-4383

Caitlin J. Bouchey − *Department of Chemistry, Washington University in St. Louis, St. Louis, Missouri 63130-4899, United States;* orcid.org/0000-0003-0729-6839

Wilson D. Bailey − *Department of Chemistry, Washington University in St. Louis, St. Louis, Missouri 63130-4899, United States;* orcid.org/0000-0001-6526-8997

Riffat Parveen − *University of South Dakota, Vermillion, South Dakota 57069, United States;* orcid.org/0000-0003-4941-7512

Complete contact information is available at: https://pubs.acs.org/10.1021/jacs.0c13470

Author Contributions

[§]V.M.K. and D.Y.S. contributed equally.

Notes

The authors declare no competing financial interest.

■ ACKNOWLEDGMENTS

We thank the National Institutes of Health (GM 47365) for financial support. X-ray diffraction data were collected using diffractometers acquired through NSF-MRI award no. CHE-1827756. Computations were performed on high performance computing systems at the University of South Dakota, funded by NSF award no. OAC-1626516.

■ REFERENCES

(1) Mirica, L. M.; Ottenwaelder, X.; Stack, T. D. P. Sructure and Spectroscopy of Copper-Dioxygen Complexes. *Chem. Rev.* **2004**, *104*, 1013−1045.

(2) Lewis, E. A.; Tolman, W. B. Reactivity of Copper-Dioxygen Systems. *Chem. Rev.* **2004**, *104*, 1047−1076.

(3) Elwell, C. E.; Gagnon, N. L.; Neisen, B. D.; Dhar, D.; Spaeth, A. D.; Yee, G. M.; Tolman, W. B. Copper−Oxygen Complexes Revisited: Structures, Spectroscopy, and Reactivity. *Chem. Rev.* **2017**, *117*, 2059−2107.

(4) Quist, D. A.; Diaz, D. E.; Liu, J. J.; Karlin, K. D. Activation of dioxygen by copper metalloproteins and insights from model complexes. *JBIC, J. Biol. Inorg. Chem.* **2017**, *22*, 253−288.

(5) Liu, J. J.; Diaz, D. E.; Quist, D. A.; Karlin, K. D. Copper(I)-Dioxygen Adducts and Copper Enzyme Mechanisms. *Isr. J. Chem.* **2016**, *56*, 738−755.

(6) (a) Solomon, E. I.; Heppner, D. E.; Johnston, E. M.; Ginsbach, J. W.; Cirera, J.; Qayyum, M.; Kieber-Emmons, M. T.; Kjaergaard, C. H.; Hadt, R. G.; Tian, L. Copper Active Sites in Biology. *Chem. Rev.* **2014**, *114*, 3659−3853. (b) Ciano, L.; Davies, G. J.; Tolman, W. B.; Walton, P. H. Bracing copper for the catalytic oxidation of C−H bonds. *Nature Catal.* **2018**, *1*, 571−577.

(7) Trammell, R.; Rajabimoghadam, K.; Garcia-Bosch, I. Copper-Promoted Functionalization of Organic Molecules: from Biologically Relevant Cu/O_2 Model Systems to Organometallic Transformations. *Chem. Rev.* **2019**, *119*, 2954−3031.

(8) Donoghue, P. J.; Tehranchi, J.; Cramer, C. J.; Sarangi, R.; Solomon, E. I.; Tolman, W. B. Rapid C−H Bond Activation by a Monocopper(III)−Hydroxide Complex. *J. Am. Chem. Soc.* **2011**, *133*, 17602−17605.

(9) Dhar, D.; Tolman, W. B. Hydrogen Atom Abstraction from Hydrocarbons by a Copper(III)-Hydroxide Complex. *J. Am. Chem. Soc.* **2015**, *137*, 1322−1329.

(10) Gagnon, N.; Tolman, W. B. $[CuO]^{+}$ and $[CuOH]^{2+}$ complexes: intermediates in oxidation catalysis? *Acc. Chem. Res.* **2015**, *48*, 2126−31.

(11) Dhar, D.; Yee, G. M.; Spaeth, A. D.; Boyce, D. W.; Zhang, H.; Dereli, B.; Cramer, C. J.; Tolman, W. B. Perturbing the Copper(III)−Hydroxide Unit through Ligand Structural Variation. *J. Am. Chem. Soc.* **2016**, *138*, 356−368.

(12) Dhar, D.; Yee, G. M.; Markle, T. F.; Mayer, J. M.; Tolman, W. B. Reactivity of the copper(III)-hydroxide unit with phenols. *Chem. Sci.* **2017**, *8*, 1075−1085.

(13) Spaeth, A. D.; Gagnon, N. L.; Dhar, D.; Yee, G. M.; Tolman, W. B. Determination of the Cu(III)−OH Bond Distance by Resonance Raman Spectroscopy Using a Normalized Version of Badger's Rule. *J. Am. Chem. Soc.* **2017**, *139*, 4477−4485.

(14) Zerk, T. J.; Saouma, C. T.; Mayer, J. M.; Tolman, W. B. Low Reorganization Energy for Electron Self-Exchange by a Formally Copper(III,II) Redox Couple. *Inorg. Chem.* **2019**, *58*, 14151−14158.

(15) Mandal, M.; Elwell, C. E.; Bouchey, C. J.; Zerk, T. J.; Tolman, W. B.; Cramer, C. J. Mechanisms for Hydrogen-Atom Abstraction by Mononuclear Copper(III) Cores: Hydrogen-Atom Transfer or Concerted Proton-Coupled Electron Transfer? *J. Am. Chem. Soc.* **2019**, *141*, 17236−17244.

(16) Bower, J. K.; Cypcar, A. D.; Henriquez, B.; Stieber, S. C. E.; Zhang, S. C(sp3)-H Fluorination with a Copper(II)/(III) Redox Couple. *J. Am. Chem. Soc.* **2020**, *142*, 8514−8521.

(17) (a) Elwell, C. E.; Mandal, M.; Bouchey, C. J.; Que, L., Jr.; Cramer, C. J.; Tolman, W. B. Carboxylate Structural Effects on the

Properties and Proton-Coupled Electron Transfer Reactivity of $[CuO_2CR]^{2+}$ Cores. *Inorg. Chem.* **2019**, *58*, 15872−15879. (b) Unjaroen, D.; Gericke, R.; Lovisari, M.; Nelis, D.; Mondal, P.; Pirovano, P.; Twamley, B.; Farquhar, E. R.; McDonald, A. R. High-Valent d(7) Ni(III) versus d(8) Cu(III) Oxidants in PCET. *Inorg. Chem.* **2019**, *58*, 16838−16848.

(18) Yang, L.; Powell, D.; Houser, R. Structural variation in copper(I) complexes with pyridylmethylamide ligands: structural analysis with a new four-coordinate geometry index, t4. *Dalton Trans.* **2007**, 955−964.

(19) Porter, T. R.; Capitao, D.; Kaminsky, W.; Qian, Z.; Mayer, J. M. Synthesis, Radical Reactivity, and Thermochemistry of Monomeric Cu(II) Alkoxide Complexes Relevant to Cu/Radical Alcohol Oxidation Catalysis. *Inorg. Chem.* **2016**, *55*, 5467−5475.

(20) Manner, V. W.; Markle, T. F.; Freudenthal, J. H.; Roth, J. P.; Mayer, J. M. The First Crystal Structure of a Monomeric Phenoxyl Radical: 2,4,6-Tri-tert-butylphenoxyl Radical. *Chem. Commun.* **2008**, 256−258.

https://dx.doi.org/10.1021/jacs.0c13470
J. Am. Chem. Soc. 2021, 143, 3295−3299